Investigation on the Recrystallization Mechanism in Warm-Rolled Ti-IF Steel

Yan-hui Guo, Zhao-dong Wang, and Li-qun Wei

The nuclei orientation, the nucleation site at the early stage of recrystallization, and the growth mechanism of the nuclei have been studied by EBSD analysis in Ti-IF steel during direct annealing after warm rolling. It is concluded that the formation of the recrystallization texture is dominated by the oriented nucleation mechanism. The recrystallized nuclei with γ-orientation emerged preferentially at the beginning of recrystallization and preferred to form in the deformed bands with γ-orientation and on the boundaries between γ- and α-orientations. The recrystallized grains first consumed their neighboring γ-oriented matrix; and then consumed the α-oriented deformed bands at the late stage of recrystallization, leading to strong γ-fiber.

1. Introduction

Interstitial-free (IF) steel is widely used due to its excellent deep drawability, high plastic strain ratio, high elongation, high hardening index, and low yield to tensile strength ratio (Ref 1, 2). It is well known that the drawability of IF steel is closely related to the texture formed during recrystallization and that a high volume fraction of near {111} components is essential for good drawability. Ferritic rolling, namely, warm rolling has been generally accepted as an effective method to improve {111} components in IF steel (Ref 3, 4).

After hot rolling in ferrite region, the texture of IF steel consists of α-fiber (⟨110⟩//RD) and γ-fiber (⟨111⟩//ND) while the recrystallization texture consists of γ-fiber. The nature of {111}⟨uvw⟩ recrystallization texture of IF steel plays a significant role in determining the planar anisotropy of the sheet properties (Ref 5, 6). Despite much research on recrystallization texture (Ref 7-12), the mechanism responsible for the formation of recrystallization texture is still a dispute.

Two main theories of recrystallization texture have been currently accepted in the wake of a controversy lasting for over 50 years. The first one, oriented nucleation theory, assumes that nuclei of specific orientations are faster in forming than those of other orientations and consequently determines the recrystallization texture (Ref 13). The second one, oriented growth theory, claims that there exist specific rotation relationships with rapid grain boundary migration.

These specific relationships between deformed and recrystallization textures are about 30°⟨110⟩ for bcc metals (Ref 14).

The present work investigates the microtexture of nuclei using electron backscatter diffraction (EBSD). The aim of the study is to gain further insight into the mechanisms of the recrystallization texture of warm-rolled IF steel.

2. Experimental Material and Method

The experimental material was obtained from industrial trial, and the chemical composition is shown in Table 1.

Slabs of 230 mm were rolled to 46 mm during rough rolling to refine austenite grains; finish rolling was performed in ferrite region with lubrication; and finishing temperature, coiling temperature, and the final thickness of slabs were 760, 440 °C, and 5 mm, respectively.

The hot bands were cooled down in air and then annealed in a hydrogen atmosphere furnace to simulate batch annealing. The annealing temperature employed in this work was 750 °C, the annealing time was 10, 20, 50 s, 2, 5, 10, 30, 50, and 60 min.

The microstructure was analyzed by optical micrograph to observe the status of grains. The samples were prepared in the usual way and etched with 4% nital. For texture measurement, mid-thickness specimens were prepared by machining and paper grinding. Macroscopic textures were measured on an X'Pert Pro x-ray diffractometer with Co K$_\alpha$ radiation (Ref 15) and three incomplete pole figures ({110}, {200}, and {211}) were obtained. Orientation distribution functions (ODFs) were then evaluated using Roe's method (Ref 16).

The metallographic photos and EBSD map of sections, which are perpendicular to the transverse direction annealing for different times, were given. Crystallographic textures were determined from the mid-thickness region of the sheets using a FEI-Quanta 600 SEM, coupled with an EBSD facility. For EBSD analysis, the specimens were mechanically polished and then electropolished in a solution of 1000 mL ethanol and 100 mL perchloric acid.

Yan-hui Guo and Li-qun Wei, Material Engineering Department Shanghai Institute of Technology, Shanghai 200235, P. R. China; and Zhado-dong Wang, The State Key Laboratory of Rolling & Automation of Northeastern University, Shenyang 110004, P. R. China. Contact e-mail: gyh415@126.com.

Table 1   Chemical composition of the test steel (mass contents in %)

Steel grade	C	Si	Mn	P	S	T_i	Nb	N	Als
Ti-IF steel	0.004	0.015.	0.12	0.007	0.007	0.068	<0.005	0.0028	0.034
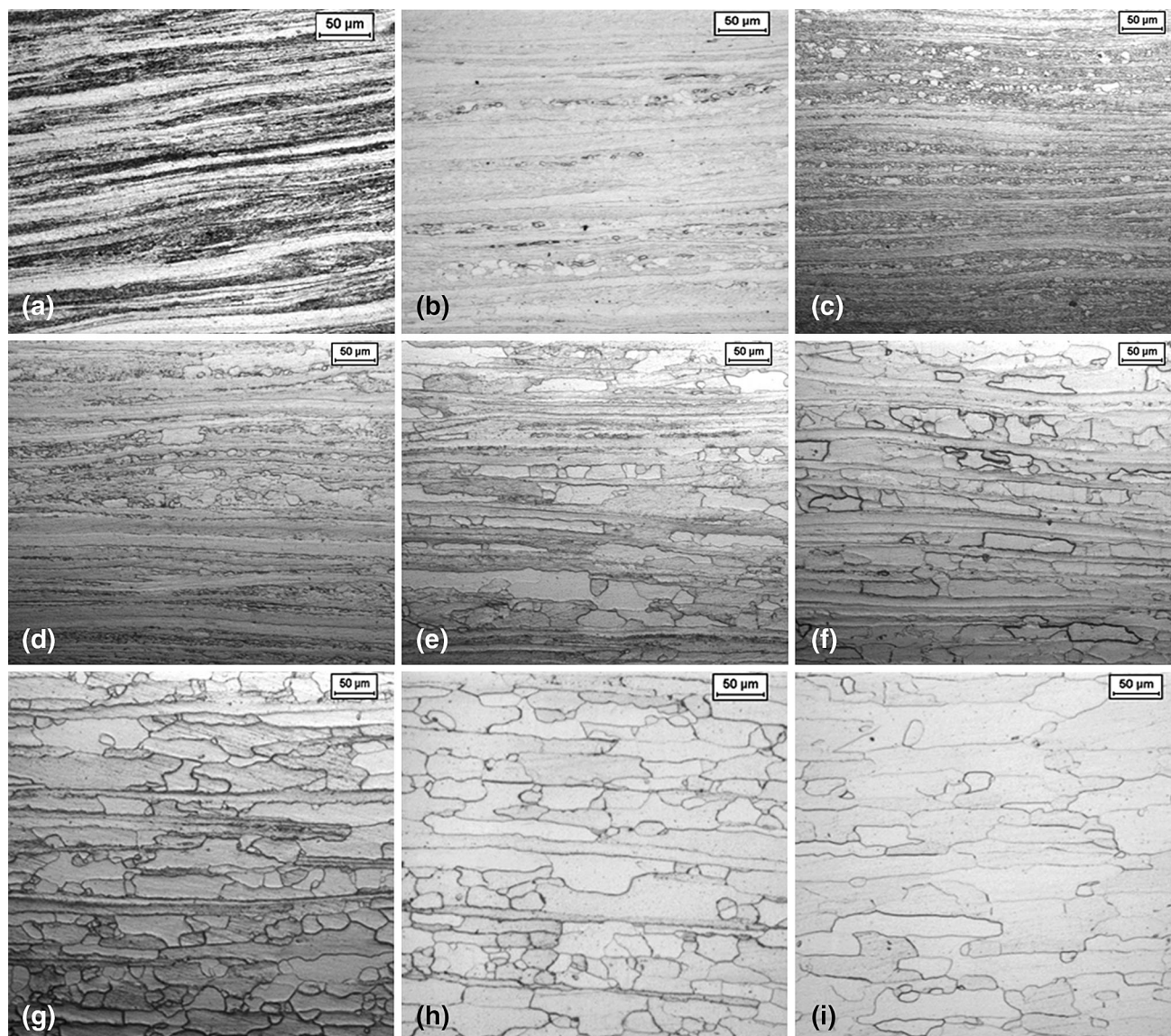
Fig. 1   Metallographs of Ti-IF steel sheets annealed at 750 °C for different times (a) warm rolled; (b) 10 s; (c) 20 s; (d) 50 s; (e) 2 min; (f) 10 min; (g) 30 min; (h) 50 min; (i) 60 min

3. Results

3.1 Microstructure

Figure 1 shows the micrographs of Ti-IF steel sheets annealed at 750 °C for different times. After warm rolling, the main microstructure is deformation bands. From the micrographs, it can be seen that the microstructure of the deformed IF steel varies from region to region. Some regions are heavily etched while some regions are lightly etched. Fragmented in-grain bands prefer to form in the heavily etched bands, while no in-grain bands form in the lightly etched bands.

After annealing for 10 s, a spot of recrystallized grains begins to appear. Figure 1b-d shows the deformed structure with few recrystallized nuclei before 50 s, and it is obvious that the recrystallized grains do not grow from the deformed grains in which they are formed until the late stage of recrystallization.

3.2 Global Texture

The ODFs shown in Fig. 2 illustrate the texture evolution during recrystallization. At the beginning of recrystallization, the texture of specimens was the same as the ferritic rolling texture. With prolongation of annealing time, the α-fiber
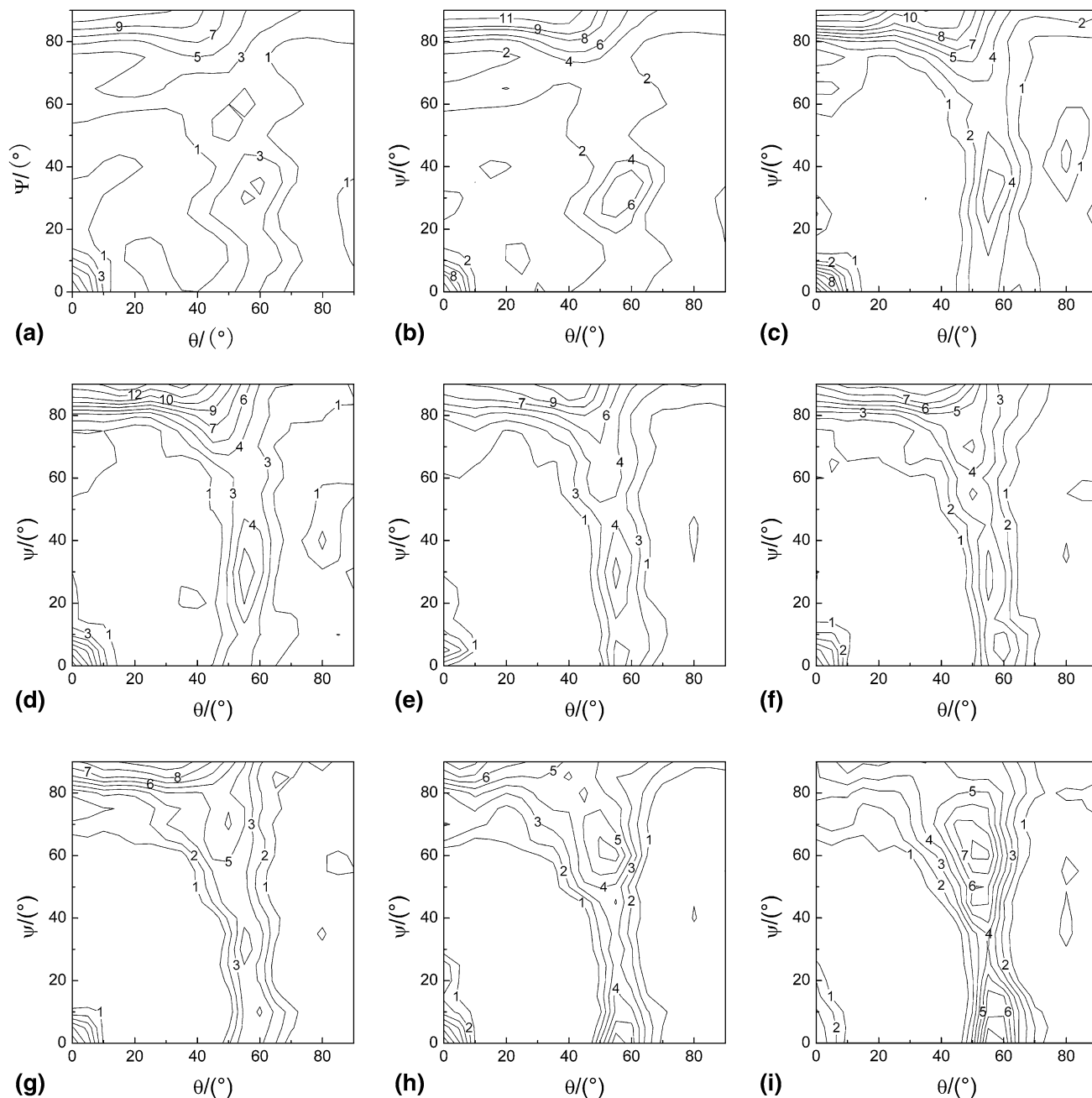
Fig. 2 Constant φ ODF sections for Ti-IF steel sheets annealed for different times (a) warm rolled; (b) 10 s; (c) 20 s; (d) 50 s; (e) 2 min; (f) 10 min; (g) 30 min; (h) 50 min; (i) 60 min

decreased gradually and a homogeneous recrystallization γ-fiber texture was eventually formed.

3.3 EBSD Analysis

Figure 3 shows the results of EBSD analysis. The orientation determination refers to Fig. 3(b). It can be seen from Fig. 3(a) that the microstructure of the ferritic rolled specimen is composed of α-orientation and γ-orientation deformation bands. The main components of the texture are {112}⟨110⟩, {001}⟨110⟩, {111}⟨110⟩, {111}⟨112⟩, and {111}⟨143⟩, consistent with the x-ray results. In the course of the EBSD study, the Kikuchi pattern changes little as the electron beam is on the straight and lightly etched bands, while the Kikuchi pattern

changes obviously as the electron beam is on the curved and heavily etched bands. This illustrates that the heavily etched bands do not belong to a single orientation, but include various orientations, and the misorientation between subgrains is large.

It can be seen from the orientation map that the straight bands belong to α-orientation and the curved bands belong to γ-orientation. The γ-oriented bands are fragmented and misorientation in the bands is large, so the Kikuchi pattern jumps. There is no fragmentation occurs in the α-oriented bands, and the misorientation in it is small, so the Kikuchi pattern changes little. In order to investigate the fragmentation in the bands, the misorientation along the rolling direction is measured, and misorientation variation of the deformed band
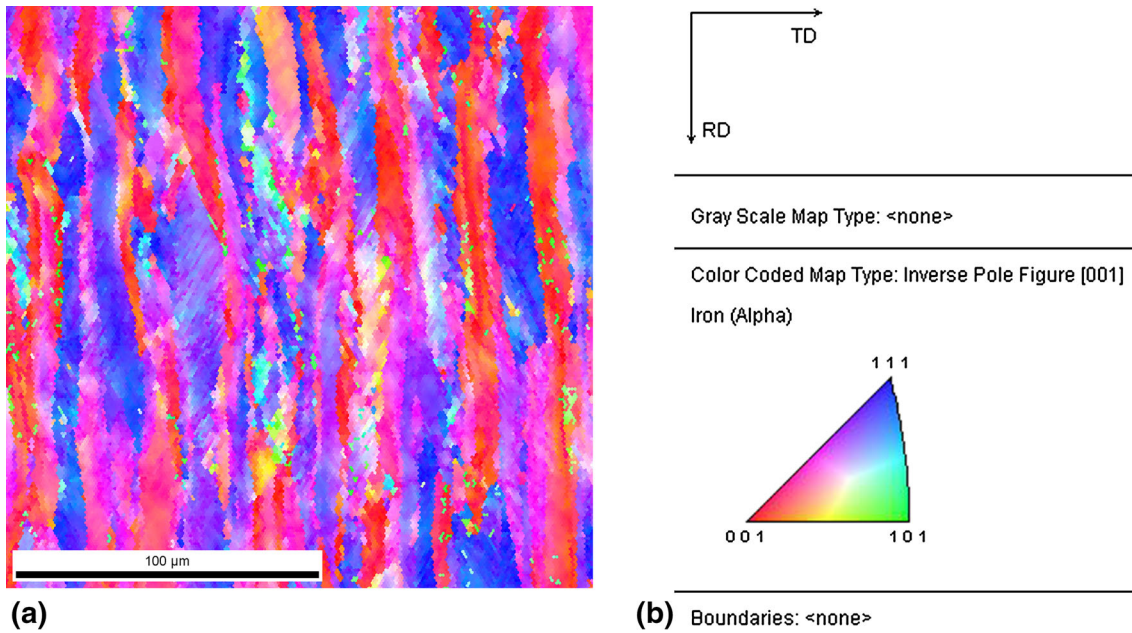
Fig. 3 Orientation map and the color-coded map for ferritic rolled Ti-IF steel sheet
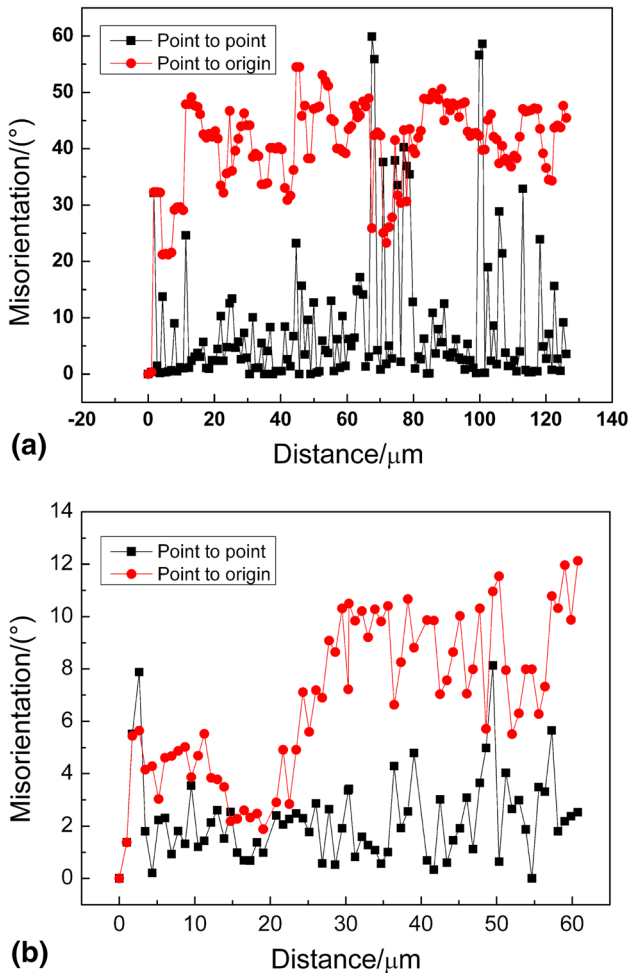
Fig. 4 Misorientation variation of the deformed band with γ-orientation and α-orientation along RD for the warm-rolled Ti-IF steel sheet (a) γ-orientation; (b) α-orientation

Fig. 5 Orientation map and constant φ ODF sections for Ti-IF steel sheet annealed for 10 s

with γ-orientation and α-orientation is shown in Fig. 4. Obviously, the misorientation in the γ-orientation bands is much larger than that in α-orientation bands. The largest misorientation in the γ-orientation bands is 60°, while it is 12° in the α-orientation bands. The fragmentation is owing to the in-grain bands, and the in-grain bands prefer to form in the grains with large Taylor factor (Ref 17, 18). For the rolling steel, the Taylor factor of the γ-orientation is the largest (Ref 19); thus, heavy fragmentation appears in the γ-orientation bands.

Figure 5 and 6 illustrate the Orientation map for Ti-IF steel sheet annealed for 10 and 20 s. It is obvious that the recrystallized grains form in the fragmented bands and the grain boundary between γ-orientation and α-orientation bands.

Figure 7 and 8 show the orientation map of specific orientations for Ti-IF steel sheet annealed for 10 and 20 s, respectively. At the early stage of the recrystallization, nuclei with {111}⟨123⟩ orientation prefer to form in the deformation bands with {111}⟨112⟩ orientation. This is in agreement with the results of cold-rolled IF steel investigated by Tse (Ref 20).
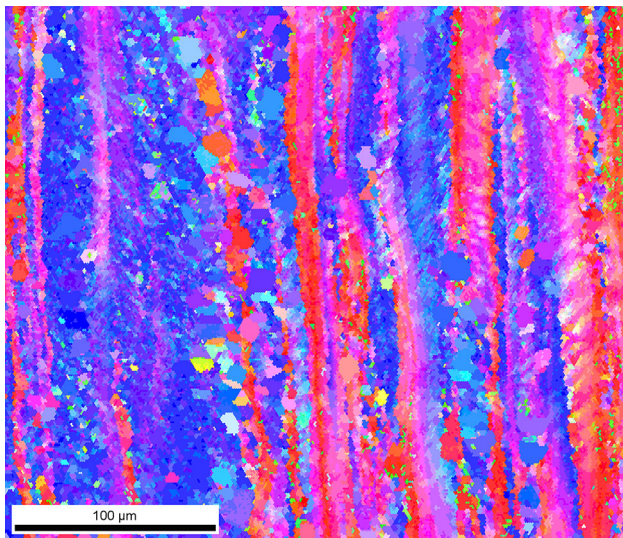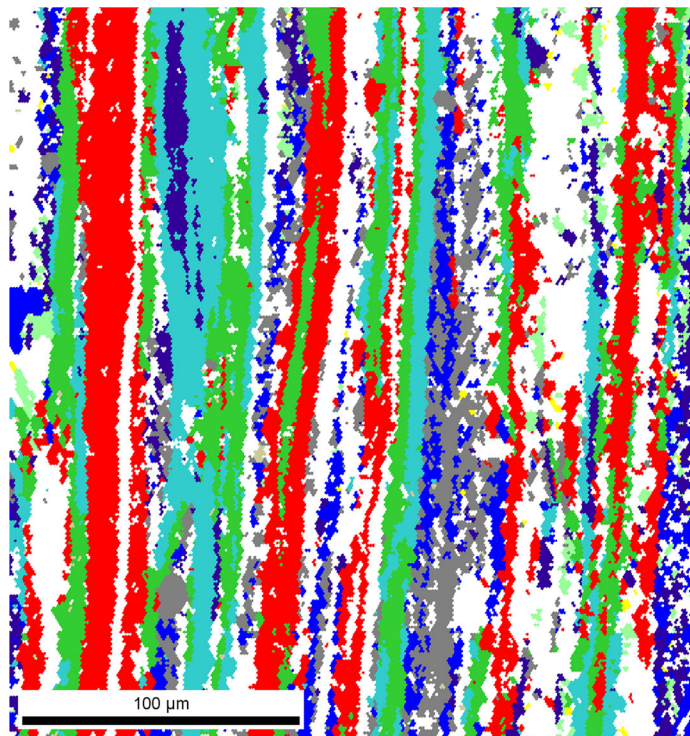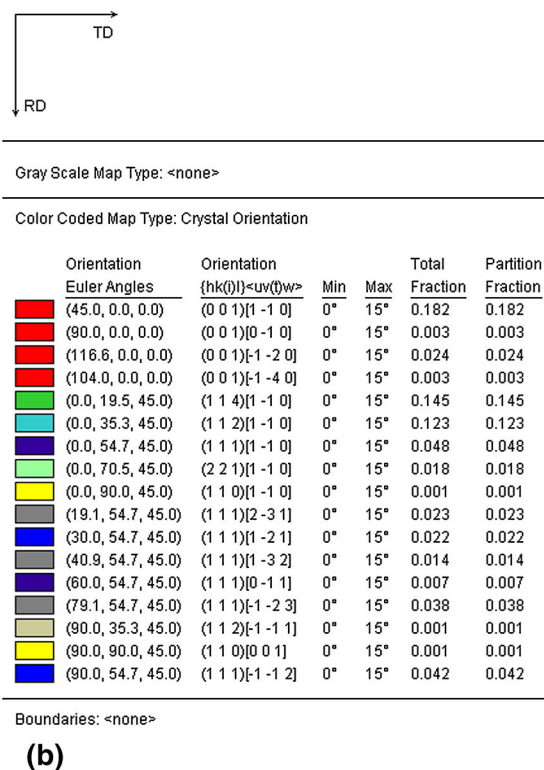
Figure 9 shows the highlight grains in EBSD map for Ti-IF steel sheet annealed for 10 s. No. 1 and 2 grains form in the interior of the γ-orientation bands, and No. 3 grain forms on the boundary between bands with γ-orientation and the other orientation. The orientation of the grains was calculated, shown in Table 2. No. 1 and 3 belong to {111}⟨123⟩. The orientation of No. 2 grain is close to {111}⟨110⟩, and the neighboring orientation is near {111}⟨112⟩.

For the specimen annealed for 20 s shown in Fig. 10, the orientation of the grains is shown in Table 3. No. 1-5 grains belong to {111}⟨110⟩ orientation. At the early stage of recrystallization, most of the nuclei belong to γ-orientation, in agreement with the main texture components after complete recrystallization; this provides that during the recrystallization, oriented nucleation is the mechanism of recrystallization.
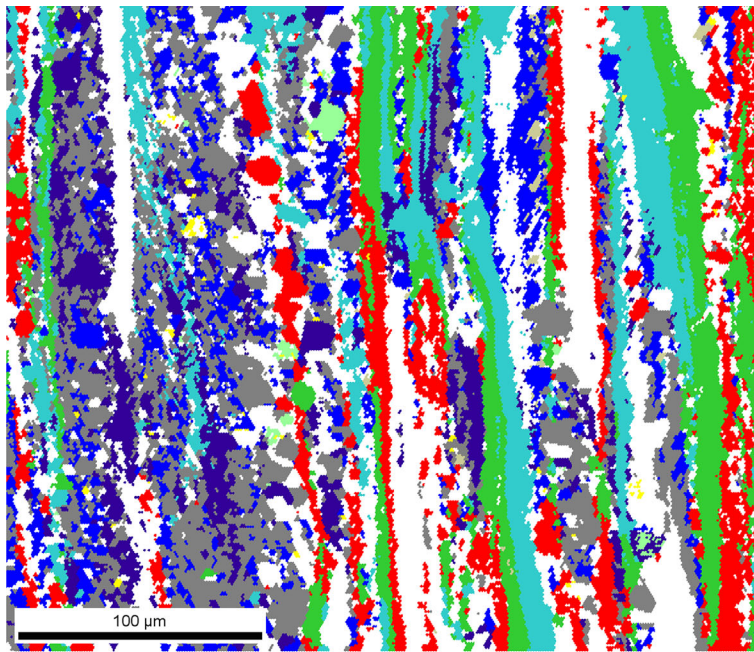
Figure 11 shows the Orientation map for Ti-IF steel sheet annealed for 50 s. It can be seen that more nuclei form after annealing for 50 s and some nuclei begin to grow up. The remaining bands are of α-orientation. Selective growth is not the mechanism of recrystallization by analyzing the orientation of the grains that have grown up. This concept is also strongly supported by the present finding that there is no significant difference between the growth rates of γ-fiber grains and that of the other orientations.

The orientation maps for Ti-IF steel sheets annealed for 2, 10, 50, and 60 min are shown in Fig. 12. With the increasing holding time, the proportion of α-orientation deformation bands gradually reduces and more and more γ-orientation grains form. After annealing for 60 min, the deformation bands disappear and pancake grains are the main microstructure. A high-angle

Fig. 6 Orientation map and constant φ ODF sections for Ti-IF steel sheet annealed for 20 s

Fig. 7 Orientation map of specific orientations for Ti-IF steel sheet annealed for 10 s

Fig. 8 Orientation map of specific orientations for Ti-IF steel sheet annealed for 20 s
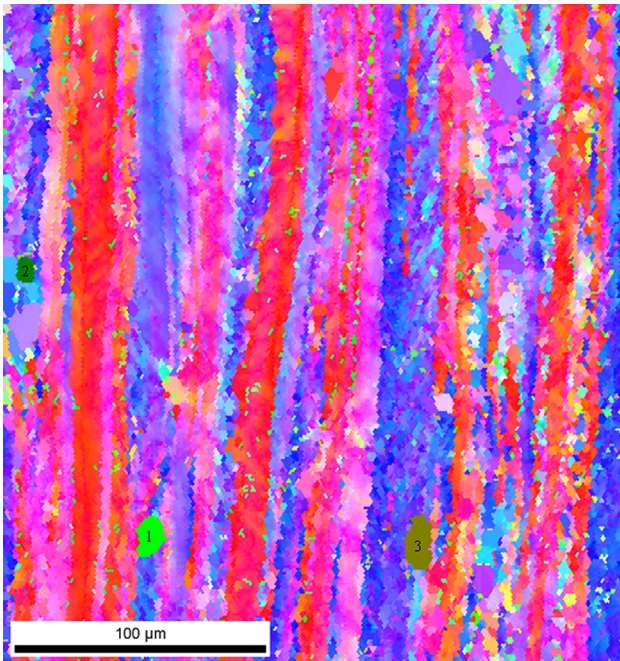

Fig. 9 The highlight grains in EBSD map for Ti-IF steel sheet annealed for 10 s

Table 2 The location and the corresponding index value of the highlighted grains in Fig. 9
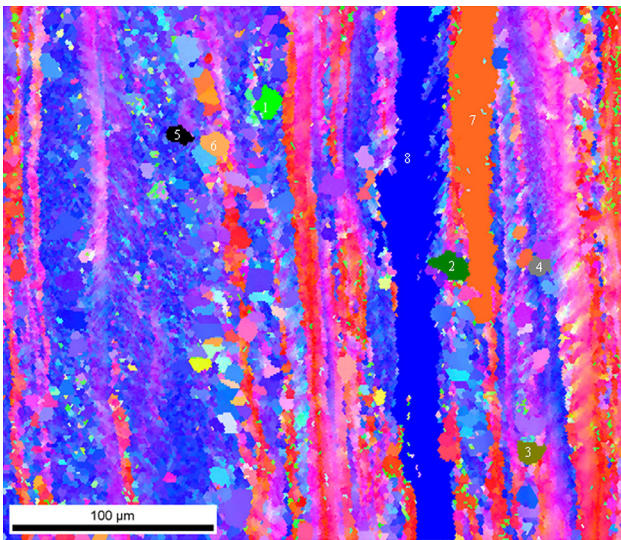
No.	Location			(hkl)[uvw]
	$\varphi_{1/(°)}$	$\varphi_{/(°)}$	$\varphi_{2/(°)}$	
1	161.1	50.8	233.7	$(\bar{4}\,\bar{3}\,4)[9\,\bar{8}3]$
2	315.6	55.1	36.6	$(576)[16\,\bar{2}\,\bar{1}\,\bar{1}]$
3	161.1	44.8	236.3	$(\bar{1}\,\bar{1}\,\bar{1})[\bar{2}3\,\bar{1}\,]$

γ-grain, and there is little driving force for consumption of α-material.

4. Discussion

One condition required for successful nucleation is a small subgrain size which facilitates subgrain coarsening. Another necessary condition is that the misorientation angle between subgrains must be large. Even if nucleation by subgrain coarsening is successful, the nuclei fail to grow if it has only low-angle grain boundaries. The misorientation angle required for the boundary to grow is around 15°. These conditions are met in the vicinity of the grain boundary, where larger lattice rotation occurs. Thus, nucleation is observed near the grain boundary of the deformed grain. These conditions are also met in the deformation bands with γ-orientation. As shown in Fig. 4, the misorientation in the γ-oriented bands is large, and it is up to 55°, which provides the necessary curvature for nucleation. In literatures (Ref 13, 21), the authors have proved that there is an internal driving force for nucleation in the fragmented γ-oriented bands.

boundary will bulge into the neighboring deformed material if it has a critical length namely L ≥ 2γ/△E, where γ is the surface energy of the interface and △E is the difference in dislocation storage across the boundary. The research of Duggan and Tse (Ref 20) supports the idea that the process of γ consuming α will occur later in the annealing cycle because several nucleation events are involved in forming one

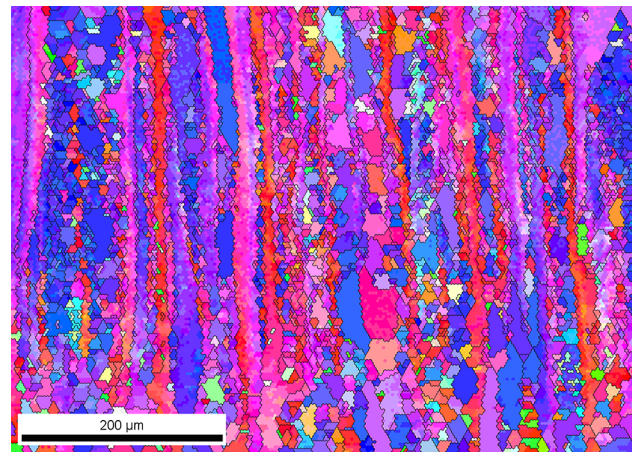**Fig. 10** The highlighted grains in EBSD map for Ti-IF steel sheet annealed for 20 s

Fig. 11 Orientation map and constant φ ODF sections for Ti-IF steel sheet annealed for 50 s

Table 3 The location and the corresponding index value of the highlighted grains in Fig. 10

No.	Location $\varphi_{1/(°)}$	$\varphi_{/(°)}$	$\varphi_{2/(°)}$	(hkl)[uvw]
1	116.6	49.6	235.1	($\overline{3}\overline{3}\ \overline{2}332$)[37 $\overline{3}$ 36]
2	138.9	48.8	219.5	($\overline{2}8\ \overline{3}336$)[39 $\overline{8}$ 23]
3	249.4	49.4	127.2	(11 $\overline{9}$12)[33 5 $\overline{3}4$]
4	10.4	47.7	314.5	($\overline{4}45$)[27224]
5	29.9	48.8	326.2	($\overline{1}52123$)[431118]
6	291.7	9.8	74.9	(6239) [27 $\overline{3}$ $\overline{4}$]
7	182.8	19.9	220.5	($\overline{1}3\ \overline{1}551$)[33 $\overline{3}2$ $\overline{1}$]
8	328.7	125.3	43.7	(262728) [18 $\overline{8}$ $\overline{9}$]

The stored energy of the main deformation texture components is classified. It is concluded that E{110}⟩E{111}⟩E{112}⟩E{100} (Ref 22). After warm rolling, few {110}-oriented bands form. The stored energy of γ-oriented bands is higher than that of bands with the other orientations. Thus, nuclei prefer to form in the interior of γ-oriented bands. On the other hand, the boundaries between different oriented bands are also the favorable place for nucleation for the energy is also higher. In addition, the nuclei like to form in the deformation matrix which has the similar orientation with them. This is the reason that γ-oriented deformation bands, the boundaries between γ-oriented and other oriented bands favor the formation of γ-oriented nuclei during recrystallization.

It can be seen from the global texture and the EBSD orientation map, that as the hot bands are annealed at a short time, the deformed texture is preserved, and a number of elongated grains exist. This may be due to the strong recovery in this condition. It is well established that for the onset of recrystallization a thermodynamic, mechanic, and kinetic instability is required. Grains with {001}⟨ll0⟩ orientation have low stored energy and small local misorientation. It is hard for grains with {001}⟨ll0⟩ orientation to recrystallize. But these grains can easily recovery, and this is the reason that strong {001}⟨110⟩ components preserve in the sample annealed at short time. Similar results are also obtained by Raabe et al. (Ref 23-25). They found that in grains with {001}⟨ll0⟩ orientation recrystallization was delayed so that strong recovery prevailed; the delay of recrystallization in grains with {001}⟨110⟩ orientation was attributed to the suppression of thermodynamic and kinetic instabilities.

Generalized recovery is the growth of a subgrain inside the parent grain with the same orientation. This mechanism has been widely observed in the lamellar microstructure. A lamellar band begins to microbulge and invades the neighboring band enabling the development of a recrystallized zone inside a grain. Hence, the zone RZ is completely recrystallized whereas the area close to the boundary (BZ) still contains lamellar bands. This subgrain growth mechanism corresponds to that proposed by Dillamore et al. (Ref 26). Dillamore defines the conditions for an elongated subgrain to grow, which are:

$$D_{Lsb}^{1} \geq 3D_{Ssb}^{2} - 2d_{Ssb}\left[\frac{4\gamma_{Lsb}^{2}}{\gamma_{Ssb}^{2}} - 1\right]^{1/2}.$$

This relation assumes the presence of a cell (potentially viable nuclei) larger than its neighboring cells with D_{Lsb}^{1} and D_{Ssb}^{2} being the lengths of the large cell (Lsb: long sub-boundaries) and the small cells (Ssb: short sub-boundaries), respectively, and d_{Ssb} the cell mean width. γ_{Lsb} is the energy value of the short sub-boundaries and γ_{Ssb} that of the long sub-boundaries.

When the cell length is smaller than 3 μm, spheroidization occurs and the microstructure becomes stabilized (the absence of longitudinal growth). This sub-structure will be consumed later, either by another subgrain or by a new recrystallized grain. When the cell length is greater than 4.7 μm, the viable subgrain grows and consumes the other neighboring subgrains whose orientation is close to that of the growing subgrain. This mechanism of generalized recovery is experimentally observed. SIBM phenomenon is not observed in this experiment. The mechanism is usually observed in the α-oriented grains, for the energy of the α-oriented bands is relatively low.

In addition, some researchers have observed that the hot-rolled grain boundaries favor the formation of FeTiP and MnS nuclei (Ref 27), and the boundaries are cumbered to migrate by the drag effect of these particles. Thus, SIBM mechanism is not
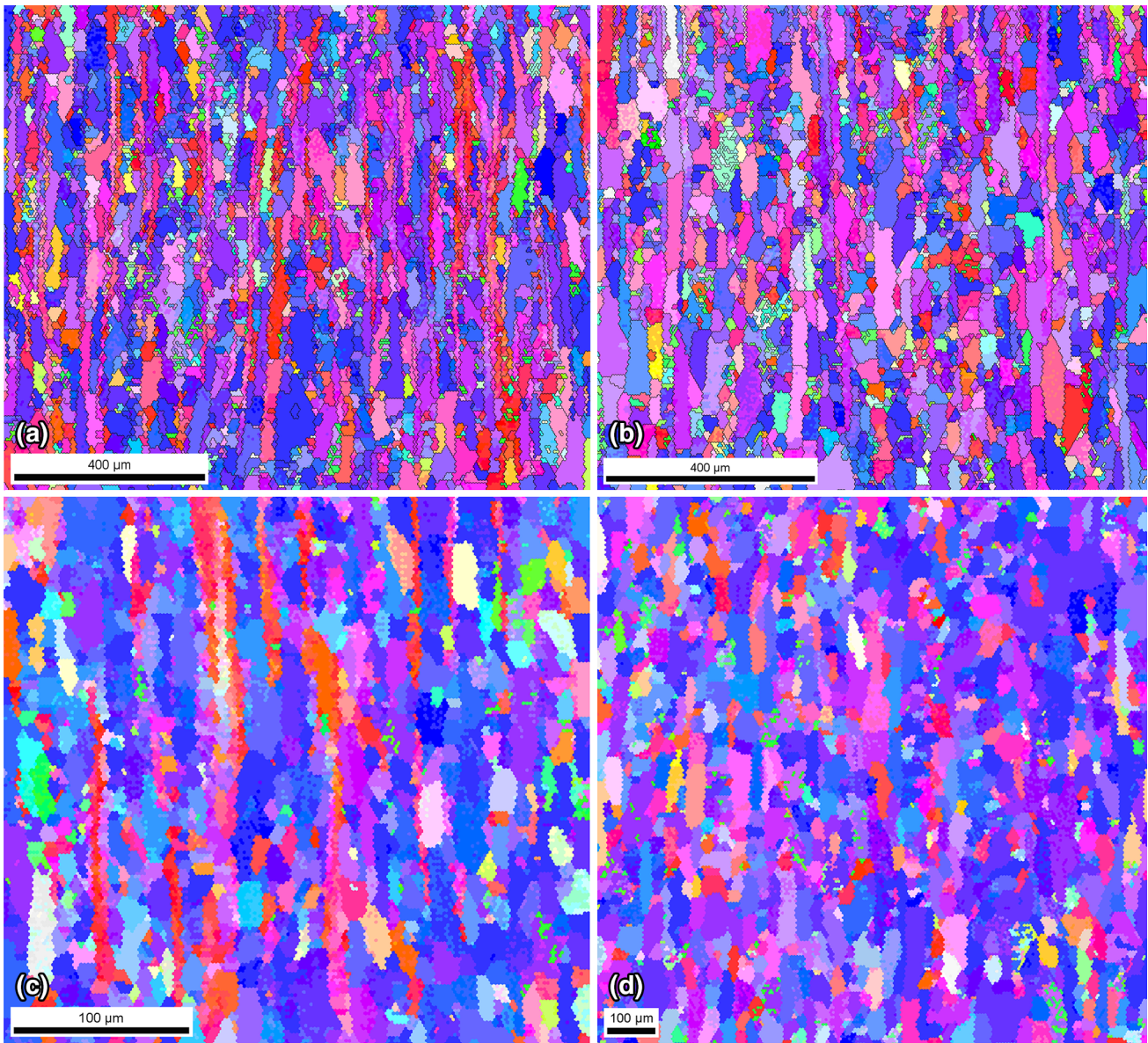
Fig. 12 Orientation map and constant φ ODF sections for Ti-IF steel annealed for different times (a) 2 min; (b) 10 min; (c) 50 min; (d) 60 min

easy to happen, the nuclei prefer to form in the γ-oriented bands, and the orientation of the nuclei is also γ-orientation.

In conclusion, if more γ-oriented bands can be obtained before annealing, there will be more sites for the γ-oriented nuclei to form, and more favorable texture components will be achieved.

5. Conclusions

(1) The recrystallized nuclei with γ-orientation emerged preferentially at the beginning of recrystallization and preferred to form in the deformed bands with γ-orientation and on the boundaries between γ- and α-orientation.

(2) The recrystallized grains first consumed their neighboring γ-oriented matrix; and then consumed the α-oriented deformed bands at the late stage of recrystallization, leading to strong γ-fiber.

(3) The formation of the recrystallization texture is dominated by the oriented nucleation mechanism.

References

1. R.K. Ray, J.J. Jonas, and R.E. Hook, Cold Rolling and Annealing Textures in Low Carbon and Extra Low Carbon Steels, *Int. Mater. Rev.*, 1994, **39**(4), p 129-172

2. M. Caul and V. Randle, Microtexture Analysis of Interstitial-Free Steel, *Mater. Charact.*, 1997, **38**, p 155-163

3. W.B. Hutchinson, Development and Control of Annealing Textures in Low-Carbon Steels, *Int. Met. Rev.*, 1984, **29**(1), p 25-42

4. G.H. Akbari, C.M. Sellars, and J.A. Whiteman, Microstructure Development during Warm Rolling of an IF Steel, *Acta Mater.*, 1997, **45**(12), p 5047-5058

5. Saitoh H, Ushtoda K, Senuma T. Structural and Textural Evolution During Subsequent Annealing of Steel Sheet Hot-Rolling in α Phase. THERMEC'88, the Iron and Steel Institute of Japan, Tokyo, 1988, p 628-635

6. Nakamura T, Esaka K. Development of Hot Rolled Steel Sheet with High R Value, *International Conference on Physical Metallurgy of Thermo Mechanical Processing of Steels and Other Metals*, THERMEC'88, the Iron and Steel Institute of Japan, Tokyo, 1988, p 644-651

7. I. Samajdar, B. Verlinden, P. Vanhoutte et al., γ-Fibre Recrystallization Texture in IF-Steel: An Investigation on the Recrystallization Mechanisms, *Mater. Sci. Eng. A*, 1997, **238**(2), p 343-350

8. M. Kiaei, R. Chiron, and B. Bacroix, Investigation of Recrystallization Mechanisms in Steels During In Situ Annealing in a SEM, *Scr. Mater.*, 1997, **36**(6), p 659-666

9. A. Samet-Meziou, A.L. Etter, T. Baudin et al., Relation Between the Deformation Sub-Structure After Rolling or Tension and the Recrystallization Mechanisms of an IF Steel, *Mater. Sci. Eng. A*, 2008, **473**(1-2), p 342-354

10. C.A.O. Shengquan, L.I. Youyuan, J. Zhang et al., EBSD Investigation on Oriented Nucleation in IF Steels, *J. Mater. Sci. Techno1.*, 2007, **23**(2), p 262-266

11. M.R. Barnett, Role of In-Grain Shear Bands in the Nucleation of ⟨111⟩//ND Recrystallization Texture in Warm Rolled Steel, *ISIJ Int.*, 1998, **38**(1), p 78-85

12. Dong Nyung Lee, The Evolution of Recrystallization Textures from Deformation Textures, *Scr. Metallurg. Mater.*, 1995, **32**(10), p 1689-1694

13. R.D. Doherty, D.A. Hughes, F.J. Humphreys et al., Current Issues in Recrystallization, *Mater. Sci. Eng.*, 1997, **A238**(2), p 219-274

14. F.J. Humphreys, M. Matherly, Recrystallization and Related Annealing Phenomena [M]. Elsevier Science Ltd. Publications, New York, 1995, p 173-178

15. L.G. Schulz, A Direct Method of Determining Preferred Orientation of a Flat Reflection Sample Using a Geiger Counter x-ray Spectrometer, *J. Appl. Phys.*, 1949, **20**, p 1030-1041

16. R.J. Roe, Description of Crystallite Orientation in Polycrystalline Materials. IIIGeneral Solution to Pole Figure Inversion, *J. Appl. Phys.*, 1965, **36**(6), p 2024-2031

17. A. Korbel and M. Sczerba, Strain Hardening of Copper Single Crystals at High Strains and Dynamical Recovery Processes, *Acta Metall*, 1982, **30**(10), p 1961-1968

18. W.B. Lee and K.C. Chan, A Criterion for the Prediction of Shear Band Angles in FCC Metals, *Acta Metallurg. Mater.*, 1991, **39**(3), p 411-417

19. L. Kestens and J.J. Jonas, Modeling Texture Change During the Static Recrystallization of Interstitial Free Steels, *Metallurg. Mater. Trans. A*, 1996, **27A**(1), p 155-164

20. Y.Y. Tse, G.L. Liu, and B.J. Duggan, Deformation Banding and Nucleation of Recrystallization in IF Steel, *Scr. Mater.*, 1999, **42**(1), p 25-30

21. I. Samajdar, B. Verlinden, and P. Vanhoutte, Texture Changes Through Grain Growth in Ti-Bearing IF-Steel Investigated by Orientation Imaging Microscopy and x-ray Diffraction, *ISIJ Int.*, 1997, **37**(10), p 1010-1016

22. H. Magnusson, D. Juul Jensen, and B. Hutchinsson, Growth Rates for Different Texture Components During Recrystallization of IF Steel, *Scr. Mater.*, 2001, **44**(3), p 435-441

23. D. Raabe, On the Orientation Dependence of Static Recovery in Low-Carbon Steels, *Scr. Maetallurg. Mater.*, 1995, **33**(5), p 735-740

24. R. Song, D. Ponge, D. Raabe, and R. Kaspar, Microstructure and Crystallographic Texture of an Ultrafine Grained C-Mn Steel and their Evolution During Warm Deformation and Annealing, *Acta Mater.*, 2005, **53**, p 845-858

25. N. Peranio, Y.J. Li, F. Roters, and D. Raabe, Microstructure and Texture Evolution in Dual-Phase Steels: Competition Between Recovery, Recrystallization, and Phase Transformation, *Mater. Sci. Eng.*, 2010, **A527**, p 4161-4168

26. I.L. Dillamore, P.L. Morris, C.J.E. Smith et al., Transition Bands and Recrystallization in Metals, *Proc. Royal Soc. Lond.*, 1972, **329**(1579), p 405-420

27. A.J. Deardo, Physical Metallurgy of Interstitial-Free Steels: Precipitates and Solutes. *International Conference on the Processing, Microstructure and Properties of IF steels*. Pittsburgh, PA. IF steels 2000 Proceedings, 2000, p 125-136